Published in final edited form as:
J Dermatol Sci. 2012 May ; 66(2): 108–118. doi:10.1016/j.jdermsci.2012.02.009.

Epidermal α6β4 integrin stimulates the influx of immunosuppressive cells during skin tumor promotion

Samar W. Maalouf[1], **Surein Theivakumar**[2], and **David M. Owens**[1,3,§]

[1]Department of Dermatology, Columbia University, College of Physicians and Surgeons, New York, NY, USA

[2]Department of Biotechnology, Columbia University, College of Physicians and Surgeons, New York, NY, USA

[3]Department and Pathology, Columbia University, College of Physicians and Surgeons, New York, NY, USA

Abstract

Background—Induction of α6β4 integrin in the differentiated epidermal cell layers in skin is a hallmark of human cutaneous SCC pathogenesis and stimulates chemically induced SCC formation in Invα6β4 transgenic mice, which exhibit persistent expression of α6β4 in the suprabasal epidermal layers. However, the molecular basis for the support of SCC development by suprabasal α6β4 is not fully understood.

Objective—We examined the relevance for suprabasal α6β4 expression in the epidermis for the recruitment of immunosuppressive leukocytes during the early stages of tumor promotion.

Methods—In this study, we made use of the Invα6β4 transgenic mouse model, which exhibits expression of α6β4 integrin in the suprabasal layers of the epidermis driven by the involucrin promoter. First, we examined protein lysates from Invα6β4 transgenic skin using a pro-inflammatory cytokine array panel. Next, we immunofluorescence labeling of murine skin sections was employed to immunophenotype tumor promoter-treated Invα6β4 transgenic skin. Finally, a M-CSF neutralizing antibody strategy was administered to resolve Invα6β4 transgenic skin inflammation.

Results—Employing the Invα6β4 transgenic mouse model, we show that suprabasal α6β4 integrin expression selectively alters the profile of secreted pro-inflammatory molecules by epidermal cells, in particular CXCL5 and M-CSF, in response to acute tumor promoter treatment. The induction of CXCL5 and M-CSF in Invα6β4 transgenic epidermis was shortly followed by an exacerbated influx of $CD200R^+$ myeloid-derived suppressor cells (MDSCs), which co-expressed the M-CSF receptor, and $FoxP3^+$ Treg cells compared to wild-type mice. As a result, the levels of activated $CD4^+$ T lymphocytes were dramatically diminished in Invα6β4 transgenic compared to wild-type skin, whereas similar levels of lymphocyte activation were observed in the peripheral blood. Finally, TPA-induced $CD200R^+$ infiltrative cells and epidermal proliferation were suppressed in Invα6β4 mice treated with M-CSF neutralizing antibodies.

§Address for correspondence: David M. Owens, Ph.D. Columbia University 1150 St. Nicholas Avenue, Room 312A New York, NY 10032 Phone: (212) 851-4544 Fax: (212) 851-4810 do2112@columbia.edu.

The authors have no conflict of interest to declare.

Conclusions—We conclude that aberrant expression of α6β4 integrin in post-mitotic epidermal keratinocytes stimulates a pro-tumorigenic skin microenvironment by augmenting the influx of immunosuppressive granular cells during tumor promotion.

Keywords

skin carcinogenesis; myeloid-derived suppressor cell; microenvironment; squamous cell carcinoma; keratinocyte

1. Introduction

Squamous cell carcinoma (SCC) is a type of nonmelanoma skin cancer derived from the epidermis of skin and has a relatively high propensity for metastasis [1,2]. Human SCCs develop along a continuum involving sequential pathological stages progressing from epidermal dysplasia to actinic keratoses to malignant SCC [1,2]. This multi-step progression to SCC is associated with many molecular changes including major alterations in membrane receptor/adhesion molecules such as integrins [3-5]. Integrins are heterodimeric cell surface glycoproteins and are receptors for extracellular matrix proteins [6,7]. Integrins play roles in a number of normal cellular processes that impact on the development of tumors, including regulation of proliferation and apoptosis, cellular motility and invasion, cell surface localization of metalloproteinases, and angiogenesis [8]. In normal epidermis, integrin expression is confined to the basal proliferative layer [6]; however, integrin expression is frequently perturbed in tumors of epidermal origin such as SCC [4,5]. Historically, the alteration that is most heavily implicated in epithelial carcinogenesis is upregulated expression of the α6β4 integrin [9]. Mechanistic studies of α6β4 have emphasized its role in promoting invasion by stimulating epithelial cell motility [10]. However, changes in α6β4 expression occur earlier during the pre-malignant stages of epithelial tumor progression. For example, suprabasal α6β4 expression is consistently observed in hyperplasic human epidermis as well as benign papillomas and is also observed in primary malignant SCCs and in metastases [11-13]. In addition, the great majority of patients who develop SCCs harboring suprabasal α6β4 expression show early relapse in those tumors [12]. In experimental mouse skin carcinogenesis, suprabasal α6β4 expression is associated with benign papillomas with a high risk of conversion to SCC [14]. Therefore, suprabasal expression of α6β4 is a hallmark throughout epidermal neoplastic progression and may be a critical determinant for the pre-malignant stages of SCC, although the mechanistic significance of suprabasal α6β4 integrin expression in human epidermal tumorigenesis is not fully understood.

Whereas strong evidence indicates that α6β4 promotes invasion of carcinoma cells, little is known regarding the importance of integrin overexpression in the early stages of tumorigenesis. It is also unclear how inappropriate expression of α6β4 in the differentiated compartment of epidermis could influence the growth and metastatic potential of undifferentiated cells in the basal layer. In prior studies to address these questions we generated a transgenic mouse model in which α6β4 is expressed in the suprabasal layers of the epidermis under the control of the involucrin promoter [15,16]. Suprabasal α6β4 expression predisposed epidermal keratinocytes to SCC and metastasis formation induced by chemical carcinogenesis. The tumorigenic effects of α6β4 were linked to a disruption in TGFβ signal transduction and TGFβ-mediated growth inhibition of basal keratinocytes via a mechanism requiring E-cadherin-dependent cell-cell adhesion and phosphoinositide 3-kinase activity [16].

However, integrins are also induced in the post-mitotic differentiated epidermal cell layers during other skin disease states, such as wound healing and psoriasis. Recent evidence

indicates that the induction of integrins in differentiated epidermal keratinocytes may perturb the recruitment and/or activation of immune cells [17]. For example, in transgenic mice expressing of α2β1 integrin in the suprabasal epidermal layers a local and systemic chronic inflammatory state is established in response to wound healing [18] whereas wound-induced inflammation is typically resolved within two weeks in wild-type mice. Suprabasal expression of β1-containing integrins is known to lead to an upregulation in mitogen-activated protein kinase signaling, which is sufficient to induce skin inflammation and inflammation-dependent spontaneous epidermal tumorigenesis [19]. Conditional deletion of α6 integrin is also associated with chronic inflammation localized to the skin [20].

The association between SCC development and inflammation has been well documented [21,22] and further substantiated in a number of transgenic murine skin carcinogenesis models [23-27], collectively indicating that chronic inflammatory stimuli represent a driving force for epidermal neoplastic cell progression. Therefore, in light of the role of chronic inflammation in the development and progression of tumors, in this study we tested the hypothesis that aberrant α6β4 integrin expression can influence the inflammatory response to orchestrate an immunosuppressive skin microenvironment conducive for the induction of SCCs.

2. Materials and methods

2.1. Transgenic and wild type mice

Invα6 [28] and Invβ4 [16] transgenic mice were kindly provided by Dr. Fiona Watt. Heterozygous Invα6 and Invβ4 transgenic mice on a homogeneous FVB/N genetic background were crossed to generate Invα6β4 double transgenic and transgene-negative wild-type (Wt) experimental mice as previously described [16]. Invα6β4 transgenic and Wt littermate mice were shaved on the dorsal surface with electric clippers and treated once with 5 nmol 12-*O*-tetradecanoylphorbol-13-acetate (TPA) (LC Laboratories) in 200 μl acetone or 200 μl acetone alone. In some cases, Invα6β4 mice received a single i.p. injection of 0.5 mg murine M-CSF neutralizing antibody (BD Biosciences) or IgG1 isotype control (BD Biosciences) as previously described [29,30] 30 min after topical acetone or TPA application. Dorsal skins were surgically excised at 4 or 24 hr following treatment and were either cryopreserved in O.C.T. medium, fixed in 10% neutral-buffered formalin and paraffin embedded, or flash frozen in liquid nitrogen for protein extraction as outlined below.

2.2. Antibodies

Antibodies were used against myeloperoxidase (Lab Vision), Foxp3 (eBioscience), F4/80 (Invitrogen), CD11b (BD Biosciences), Gr-1 (BD Biosciences), CD4 (BioLegend), CD69 (BioLegend), CD200R1 (R&D Systems), M-CSFR (R&D Systems), CXCR2 (R&D Systems) and Ki67 (Millipore).

2.3. Cytokine Arrays

For each mouse, epidermal protein lysates were generated from frozen dorsal skin scrapes that were homogenized in Lysis Buffer (RayBiotech). For each lysate, a total of 500 μg of protein was hybridized to the Mouse Inflammation Antibody Array 1 as per manufacturer instruction (RayBiotech) (Supplementary Fig. S1A). Each experimental group was run in duplicate. For densitometric analysis, individual cytokine values were corrected by subtraction from the average background reading for each membrane followed by normalization to the average positive control signal (n = 6 positive control readings per membrane). Average-corrected cytokine concentrations (n = 2 cytokine readings per membrane) were statistically compared between TPA- or acetone-treated Invα6β4 transgenic versus Wt mice (Student's *t* test; $P < 0.05$).

2.4. Tissue staining

Skin cryosections were fixed in acetone, blocked and probed with primary antibodies followed by detection with species-specific Alexa Fluor-conjugated secondary antibodies (Invitrogen) as previously described [16,31]. Formalin fixed, paraffin-embedded sections were de-waxed, blocked and probed with primary antibodies overnight at 4° C followed by histochemical detection using DAB chromagen (Biogenex) as previously described [16,31]. For proliferation analysis, Ki67-stained skin sections were observed using Zeiss Axioplan 2 microscope with fluorescent capability (data not shown). Six slides were analyzed per mouse and minimum of 1000 DAPI-positive basal cells were counted per mouse after which the same area was counted for $Ki67^+$ cells. For detection of mast cells, paraffin skin sections were de-waxed and stained with 0.1% toluidine blue (Fisher Scientific). Bright field images were captured on a Zeiss Axioplan 2 microscope and fluorescent images were captured on a Zeiss LSM 5 Exciter confocal microscope.

2.5. Immune infiltrate analysis

For quantification of immune infiltrates, DAPI positive nuclei of positively stained cells were counted in the whole skin tissue and the number was divided by the length of the tissue in millimeters. For all cell types, infiltrates were counted in a total of 6 skin sections per mouse and three mice per group unless otherwise stated. The results were represented as average ± standard deviation and were statistically compared between TPA- or acetone-treated Invα6β4 transgenic versus Wt mice (Student's *t* test; $P < 0.05$).

2.6. T lymphocyte activation assay

Peripheral blood T lymphocyte activation in response to CD3/CD28 antibody stimulation was conducted as previously described [32]. Briefly, peripheral blood samples were isolated from Invα6β4 transgenic and Wt mice 24 hr following 5 nmol TPA or acetone vehicle treatment. Following red blood cell lysis, total live cell counts were obtained using a Countess cell counter (Invitrogen) and equal numbers of leukocytes were incubated with Dynal bead-conjugated CD3/CD28 antibodies according to manufacturer instruction (Invitrogen) for 5 hr at 37°C. After which, cells were washed and stained with APC-conjugated CD4 and PE-conjugated CD69 antibodies. Labeled cells were subjected to flow cytometry performed on a LSRII FACS scanner equipped with 407nm, 488nm, 633nm and UV excitation lines (BD Biosciences) and data were analyzed using the FlowJo Flow Cytometry Analysis software (Tree Star, Inc., Version 6.3.3). First, lymphocytes were gated by size based on forward and side scatter followed by gating DAPI-negative live cells. From the live cell population the percentage of $CD4^+$ cells that were also $CD69^+$ were statistically compared between non-stimulated and stimulated Invα6β4 transgenic versus Wt mice using a Student's *t* test ($P < 0.05$) ($n = 3$ mice per group).

3. Results

3.1. Augmented dermal infiltrate and secretion of pro-inflammatory proteins in Invα6β4 transgenic skin

Invα6β4 transgenic mice are more susceptible to TPA-induced epidermal proliferation and squamous cell carcinogenesis, which is due in part to defective TGF-β growth inhibition in epithelial keratinocytes [16]. To explore additional roles for aberrant epidermal α6β4 expression, we characterized the inflammatory response to acute TPA tumor promoter treatment in Invα6β4 mice compared to Wt littermate mice. In H&E-stained histological sections, similar levels of infiltrative cells were observed between vehicle-treated Invα6β4 and Wt mouse skin (Figure 1A-B). However, 24 hr following a single topical application of TPA a dramatic increase in the frequency of dermal inflammatory cells was apparent in

Invα6β4 skin compared to Wt skin (Figure 1C-D) suggesting that suprabasal α6β4 expression may predispose the skin to heightened inflammatory recruitment in response to tumor promotion.

To begin to assess this idea, we utilized Inflammation Antibody Arrays to assess the levels of 40 pro-inflammatory cytokines or chemokines acutely induced in the epidermis of Invα6β4 mice at 4 hr (prior to the infiltration of dermal leukocytes) or 24 hr following a single application of TPA (Supplementary Figure S1A). On average, a larger sub-set of the pro-inflammatory molecules assayed (48%) were induced at 4 hr following TPA treatment in Invα6β4 epidermis compared to just 13% in Wt epidermis (Supplementary Figure S1B) indicating that Invα6β4 epidermis was more sensitive to TPA-induced acute changes in the expression of pro-inflammatory proteins. We found the levels of four proteins to be substantially altered in Invα6β4 compared to Wt epidermis. Macrophage inflammatory protein 1-γ (MIP1γ), which is important for the recruitment of monocytes and $CD4^+$ and $CD8^+$ T lymphocytes [33], exhibited three- to four-fold lower steady state levels in Invα6β4 epidermis but was induced at similar levels in Wt and Invα6β4 mice 4h after TPA treatment (Figure 1E). At 24 hr after TPA treatment the levels of MIP1γ were again significantly lower in Invα6β4 skin (Figure 1E). Monocyte chemotactic protein-1 (MCP1), which recruits monocytes and macrophages [34], was also induced at similar levels by TPA in Invα6β4 and Wt skin after 4 hr while significantly higher (three-fold) levels persisted in Invα6β4 skin at 24 hr following TPA treatment (Figure 1F). Interestingly, two inflammatory molecules, LPS-induced CXC chemokine (LIX), a chemokine that recruits neutrophils [35,36], and Macrophage colony stimulating factor (M-CSF), known to recruit monocytes and macrophages [37], were both exclusively induced at 4 and 24 hr in Invα6β4 skin in response to TPA treatment (Figure 1G-H). Collectively, these results correlate an exacerbated immune infiltrate with the highly selective induction of two pro-inflammatory molecules, LIX and M-CSF, in Invα6β4 skin in response to acute tumor promoter treatment and prior to the influx of infiltrative leukocytes. These findings suggest that the sensitivity of Invα6β4 mice to SCC formation may correlate with perturbed activity of myeloid and/or lymphoid cell lineages infiltrating the skin.

3.2. Analysis of myeloid cell infiltration in TPA-treated Invα6β4 skin

To begin to characterize the phenotype of dermal infiltrative cells in Invα6β4 skin, we probed vehicle- and TPA-treated Invα6β4 and Wt skin sections with antibodies against myeloperoxidase (MPO) as a means to detect infiltrating monocytes and polymorphonuclear leukocytes. Consistent with H&E staining (Figure 1), similar levels of MPO^+ cells were detected between acetone vehicle-treated Invα6β4 and Wt skin (Figure 2A,C). However, a three- to four-fold increase in the number of MPO^+ cells were observed in Invα6β4 skin 24 hr post TPA treatment compared to Wt skin (Figure 2B,D,E). Next, we analyzed Invα6β4 and Wt skin sections for the presence of mast cells as determined by toluidine blue staining. No differences in mast cell numbers were observed between Invα6β4 and Wt skin either treated with vehicle or TPA, and TPA treatment did not appear to influence the numbers of dermal mast cells present in the skin (Figure 2F-J). The numbers of macrophages infiltrating the dermis were also assessed by F4/80 immunofluorescence labeling. An increase in $F4/80^+$ macrophages was observed 24 hr post TPA treatment (Figure 2L,N) compared to steady state levels in Invα6β4 and Wt skin (Figure 2K,M); however, no differences in the influx of $F4/80^+$ macrophages were observed between Invα6β4 and Wt skin (Figure 2O). Collectively, these results indicate that the $F4/80^+$ macrophages significantly contribute to the MPO^+ dermal cell infiltrate in TPA-treated Invα6β4 and Wt skin but additional myeloid populations may be selectively recruited by TPA in Invα6β4 skin.

We previously identified the CD200 receptor, CD200R1, as a marker of $CD11b^+Gr\text{-}1^+$ myeloid-derived suppressor cells (MDSCs), which were a major population of infiltrative

immunosuppressive cells in murine cutaneous benign papillomas and squamous cell carcinomas [38]. However, whether MDSCs infiltrate skin during the earlier stages of tumor promotion and contribute to the cutaneous pre-neoplastic microenvironment has not been determined. Therefore, we probed sections of Invα6β4 and Wt skin to determine whether $CD11b^+Gr\text{-}1^+CD200R1^+$ MDSCs may be preferentially infiltrating Invα6β4 skin in response to TPA. Very few but comparable levels of $CD11b^+CD200R1^+$ cells were present in the dermis of vehicle-treated Invα6β4 and Wt skin (Figure 3A,E). However, these $CD200R1^+$ cells did not co-express Gr-1 in either vehicle-treated Invα6β4 or Wt skin (Figure 3C,G) consistent with the finding that CD200R1 is primarily expressed on macrophages in normal skin [39]. Following TPA treatment a marked increase in $CD11b^+CD200R1^+$ cells were present in the dermis of Invα6β4 and Wt skin (Figure 3B,F); however, there were two fundamental differences in the infiltrate in Invα6β4 skin. First, the level of $CD11b^+CD200R1^+$ infiltrate was dramatically higher in TPA-treated Invα6β4 compared to Wt skin (Figure 3B,F). Second, the phenotype of most $CD11b^+CD200R1^+$ cells infiltrating Invα6β4 skin was distinct to that infiltrating Wt skin. Very few $CD200R1^+$ dermal cells co-expressed Gr-1 in TPA-treated Wt skin (Figure 3D), while the majority of $CD200R1^+$ cells co-expressed CD11b and Gr-1 in TPA-treated Invα6β4 skin (Figure 3F,H) suggesting that the presence of suprabasal α6β4 may preferentially promote the recruitment of $CD11b^+Gr\text{-}1^+CD200R1^+$ MDSCs to the skin.

3.3. Infiltrating $CD200R1^+$ myeloid cells co-express the M-CSF receptor

To determine whether there may be a direct link between either CXCL5 or M-CSF release (Figure 1) and the influx of immunosuppressive dermal cells, we probed Invα6β4 skin sections with antibodies against CXCR2 (CXCL5 receptor) or the M-CSF receptor in conjunction with CD200R1 as a marker for infiltrative MDSCs (Figure 3) [38]. Very few of the dermal infiltrative cells exhibited positive immunoreactivity for CXCR2, presumably neutrophils [40], in either Invα6β4 or Wt TPA-treated skin sections, and none of the $CXCR2^+$ cells co-labeled with CD200R1 antibodies (data not shown). In contrast, immunopositive staining for M-CSFR was prominently featured on infiltrative dermal cells in TPA-treated Invα6β4 and Wt skin sections (Figure 4B,E), and the majority of $CD200R1^+$ infiltrative cells co-expressed the M-CSFR (Figure 4C,F). Moreover, the differences in distribution of dermal $M\text{-}CSFR^+$ cells between TPA-treated Invα6β4 and Wt skin sections correlated with the numbers of infiltrative $CD200R1^+$ MDSCs (Figure 3). These results suggest that epidermal-derived M-CSF release may play a key role in regulating an immunosuppressive skin microenvironment.

3.4. Enhanced recruitment of $FoxP3^+$ Tregs in Invα6β4 skin

Immunosuppressive regulatory T cells (Tregs) are also implicated in cutaneous SCC progression [41]. Therefore, we analyzed Invα6β4 and Wt skin for the presence of infiltrating Tregs, as determined by FoxP3 positive immunoreactivity, in response to TPA treatment. $FoxP3^+$ Tregs were present in the dermis of vehicle-treated Invα6β4 and Wt skin at comparable albeit low numbers (Figure 5A,B). The frequency of dermal $FoxP3^+$ Tregs increased in response to TPA treatment in Invα6β4 and Wt skin (Figure 5C,D); however, approximately 2-fold more $FoxP3^+$ Tregs were detected in Invα6β4 compared to Wt skin (Figure 5E).

3.5. Local but not systemic immune suppression in TPA-treated Invα6β4 mice

To determine whether the augmented recruitment of $CD11b^+Gr\text{-}1^+CD200R1^+$ myeloid and $FoxP3^+$ Treg dermal cells was associated with systemic suppression of T lymphocytes in Invα6β4 mice, we harvested peripheral blood leukocytes from Invα6β4 and Wt mice 24 hr following a single application of TPA and compared the activation levels of $CD4^+$ lymphocytes upon stimulation with CD3/CD28 antibodies [32]. Following a single

application of 5 nmol TPA, equal numbers of heterogeneous peripheral blood cells were stimulated with CD3 and CD28 antibodies and analyzed by flow cytometry to quantify the percentage of activated $CD4^+$ T lymphocytes as measured by CD69 surface levels [32]. In non-stimulated cells, very few $CD4^+$ T lymphocytes co-expressed $CD69^+$ in either Invα6β4 (4.5%) or Wt mice (2.2%) with no significant difference between each group (Student's *t* test, $p = 0.29$) (Figure 5F-H). A marked increase in $CD4^+CD69^+$ T lymphocytes was observed in both Invα6β4 (76.1%) and Wt mice (77.8%) in CD3/CD28-stimulated cells; however, no discernable difference in the percentages of $CD4^+$ T lymphocyte activation was observed (Student's *t* test, $p = 0.74$) (Figure 5F-H) indicating that effects of suprabasal α6β4 expression do not lead to the systemic suppression of $CD4^+$ T lymphocytes in response to acute TPA treatment.

To assess whether suprabasal α6β4 expression may lead to localized suppression of skin-infiltrating T lymphocytes, we co-labeled skin sections from TPA-treated Invα6β4 and Wt mice with antibodies against CD4 and CD69. The frequency of $CD4^+CD69^+$ versus $CD4^+CD69^-$ T lymphocyte subpopulations as detected by immunostaining in histological sections of head and neck SCC has been effectively utilized as a marker for cancer patients with higher proportions of activated $CD4^+CD69^+$ T lymphocytes correlating with good patient prognosis [42]. Similar levels of infiltrative $CD4^+$ T lymphocytes were detected in TPA-treated Wt skin compared to Invα6β4 skin (Figure 5I,J). We observed approximately 30-40% of $CD4^+$ cells to co-express CD69 in TPA-treated Wt skin; however, no CD69 co-expression was observed in $CD4^+$ cells in TPA-treated Invα6β4 skin ($n = 5$ sections/mouse, 3 mice/group) (Figure 5K). Collectively, these results indicate that suprabasal α6β4 is associated with localized but not systemic suppression of $CD4^+$ T lymphocytes during the early stages of skin tumor promotion.

3.6. Suppression of TPA-induced skin infiltration and proliferation by administration of M-CSF neutralizing antibody

To determine the significance of augmented M-CSF levels observed in TPA-treated Invα6β4 skin, mice were administered a M-CSF neutralizing antibody or IgG isotype control as previously described [29,30] shortly after topical TPA application as a means of blocking M-CSFR signaling and MDSC infiltration. Pharmacological inhibition of M-CSFR signaling has shown to be an effective means of inhibiting the recruitment of tumor-infiltrating myeloid cells, including MDSCs, in orthotopic tumor models [43]. Invα6β4 mice received a topical application of TPA or acetone vehicle and 30 min later received a single i.p. injection of 0.5 mg M-CSF neutralizing antibody or IgG isotype control. Skins were harvested 24 hr following TPA treatment and analyzed for the levels of $CD200R^+$ infiltrating cells as a marker of MDSCs and epidermal proliferation. No differences in histological appearance (Figure 6A,B) or in the levels of $CD200R1^+$ (Figure 6E,F,I) or $Ki67^+$ (Figure 6G,H,J) cells were observed in vehicle-treated skin from mice receiving M-CSF versus IgG control antibodies. Qualitative analysis of H&E-stained skin sections indicated that the extent of TPA-induced generalized skin inflammation and epidermal hyperplasia was reduced in Invα6β4 mice receiving M-CSF compared to IgG control antibody (Figure 6C,D). To substantiate these observations, we probed skin sections from each group with CD200R1 antibodies to detect MDSCs [38] and Ki67 to mark proliferating keratinocytes. On average, M-CSF antibody administration suppressed the levels of $CD200R1^+$ infiltrating cells by 40-50% compared to IgG isotype control treatment (Figure 6G,H,I). In addition, the reduction in $CD200R1^+$ infiltrating cells in M-CSF antibody-treated Invα6β4 mice was associated with a two- to three-fold decrease in proliferating epidermal cells as determined by Ki67 immunostaining (Figure 6J and data not shown).

4. Discussion

The strong association between tumor development and chronic inflammation has been well documented; however, the specific role that epidermal keratinocytes in the post mitotic layers play in the development of a pro-inflammatory yet immunosuppressive skin microenvironment is not fully understood. In this study, we focused on the pro-inflammatory effects of early stage TPA tumor promotion in the skin to begin to decipher a molecular basis for the effects suprabasal expression of α6β4 integrin on the regulation of an immunosuppressive skin microenvironment.

We found two pro-inflammatory molecules, CXCL5 and M-CSF, were acutely induced in response to a single treatment of TPA, which was followed by an influx of immunosuppressive dermal infiltrative cells in Invα6β4 transgenic to a much greater extent than that observed in Wt skin. In response to TPA treatment, we observed a similar influx of $F4/80^+$ macrophages between Invα6β4 and Wt skin but a preferential influx of $CD11b^+Gr\text{-}1^+CD200R1^+$ infiltrating myeloid cells in Invα6β4 skin with the latter matching the phenotype of tumor infiltrating MDSCs [38,44]. As a result, the activation of $CD4^+$ T lymphocytes is diminished in TPA-treated Invα6β4 transgenic skin, a phenomenon that may contribute to the susceptibility of these mice to chemically-induced SCC formation [16]. However, our data does not speak to the activation status of other anti-tumor leukocyte sub-populations such as natural killer cells, $\gamma\delta^+$ dendritic epidermal T lymphocytes or $CD8^+$ T lymphocytes. Our findings using a mouse model exhibiting forced expression of suprabasal α6β4 integrin expression suggests that transient increases in the influx of immunosuppressive cells are present in the skin in response to acute inflammatory stimuli; however, sustained suprabasal expression of endogenous α6β4 integrin may be required for pathological stages of skin inflammation that stimulate tumor formation. This concept fits well with the sustained influx of $CD200R^+$ stromal cells that we previously observed in wild-type papillomas after the cessation of TPA [38].

We observed expression of the M-CSF receptor in a large population of skin infiltrative cells linking the induction of M-CSF in Invα6β4 epidermis to the development of an immunosuppressive skin microenvironment. M-CSF is well known for its role in the development of macrophages and the M-CSF receptor is expressed by macrophages, Langerhans cells and dendritic cell populations in the skin during homeostasis [45]. The induction of M-CSF has been previously reported both in normal epidermal keratinocytes and in solid tumors. M-CSF expression is highly induced in epidermal keratinocytes following UVB exposure in a mutant mouse model of cutaneous lupus where M-CSF release is critical for the recruitment of pro-apoptotic macrophages [46]. The presence of the M-CSF receptor on tumor infiltrating MDSCs has been previously reported [47,48] and MDSC tumor infiltration and MDSC-mediated angiogenesis can be blocked with pharmacological inhibitors of the M-CSFR signaling cascade [43]. The novelty of our study is based on our finding that M-CSF induction in the epidermis is an early event prior to the onset of dermal infiltration and, in as much, may represent initiating event in the development of an immunosuppressive skin microenvironment during epithelial carcinogenesis. In addition, while MDSC function has been largely investigated following primary tumor formation, we show that both MDSC and Treg immunosuppressive subpopulations inhabit the skin prior to any significant clonal expansion of initiated cells. Under conditions where the skin is damaged or diseased our findings indicate that recruitment of the immunosuppressive properties of MDSCs may be one of the earliest facilitators of α6β4-mediated epithelial tumor formation. Therefore, our results warrant further studies to determine the functional significance of M-CSFR expression by infiltrating myeloid cells in a natural skin carcinogenesis setting and suggest that neutralizing antibodies or pharmacological inhibitors

of the MCSF-R signaling pathway may represent prophylactic strategies against SCC development.

Supplementary Material

Refer to Web version on PubMed Central for supplementary material.

Acknowledgments

We thank Yan Lu (NIH SDRC Tissue Phenotyping Core Facility) for technical assistance and Raphael Clynes (CUMC Department of Medicine) for assistance with T lymphocyte activation assays.

Funding source: This work was supported by NIH R01CA114014 (DMO, ST) and NYSTEM N08G-335 (DMO, SM) research grants.

References

1. Bachelor MA, Owens DM. Squamous cell carcinoma of the skin: current strategies for treatment and prevention. Curr Cancer Ther Rev. 2009; 5:37–44.
2. Murad A, Ratner D. Primary care: cutaneous squamous-cell carcinoma. New Eng J Med. 2001; 344:975–83. [PubMed: 11274625]
3. Quynh-Thu L, Giaccia AJ. Therapeutic exploitation of the physiological and molecular genetic alterations in head and neck cancer. Clin Cancer Res. 2003; 9:4287–95. [PubMed: 14555497]
4. Mizejewski GJ. Role of integrins in cancer: survey of expression patterns. Proc Soc Exp Biol Med. 1999; 222:124–38. [PubMed: 10564536]
5. Abraham MT, Kuriakose A, Sacks PG, Yee H, Chiriboga L, Bearer EL, Delacure MD. Motility-related proteins as markers for head and neck squamous cell cancer. Laryngoscope. 2001; 111:1285–9. [PubMed: 11568556]
6. Watt FM. Role of integrins in regulating epidermal adhesion, growth and differentiation. EMBO J. 2002; 21:3919–26. [PubMed: 12145193]
7. Hynes RO. Integrins: bidirectional, allosteric signaling machines. Cell. 2002; 110:673–87. [PubMed: 12297042]
8. Hood JD, Cheresh DA. Role of integrins in cell invasion and migration. Nat Rev Cancer. 2002; 2:91–100. [PubMed: 12635172]
9. Rabinovitz I, Mercurio AM. The integrin α6β4 and the biology of carcinoma. Biochem Cell Biol. 1996; 74:811–21. [PubMed: 9164650]
10. Mercurio AM, Rabinovitz I, Shaw LM. The α6β4 integrin and epithelial cell migration. Curr Opin Cell Biol. 2001; 13:541–5. [PubMed: 11544021]
11. Kimmel KA, Carey TE. Altered expression in squamous carcinoma cells of an orientation restricted epithelial antigen detected by monoclonal antibody A9. Cancer Res. 1986; 46:3614–23. [PubMed: 3708592]
12. Wolf GT, Carey TE, Schmaltz SP, McClatchey KD, Poore J, Glaser L, Hayashida DJ, Hsu S. Altered antigen expression predicts outcome in squamous cell carcinoma of the head and neck. J Natl Cancer Inst. 1990; 82:1566–72. [PubMed: 2119437]
13. Van Waes C, Surh DM, Chen Z, Kirby M, Rhim JS, Brager R, Sessions RB, Poore J, Wolf GT, Carey TE. Increase in suprabasilar integrin adhesion molecule expression in human epidermal neoplasms accompanies increased proliferation occurring with immortalization and tumor progression. Cancer Res. 1995; 55:5434–44. [PubMed: 7585613]
14. Tennenbaum T, Weiner AK, Belanger AJ, Glick AB, Hennings H, Yuspa SH. The suprabasal expression of α6β4 integrin is associated with a high risk for malignant progression in mouse skin carcinogenesis. Cancer Res. 1993; 53:4803–10. [PubMed: 8402665]
15. Carroll JM, Albers KM, Garlick JA, Harrington R, Taichman LB. Tissue- and stratum-specific expression of the human involucrin promoter in transgenic mice. Proc Natl Acad Sci USA. 1993; 90:10270–4. [PubMed: 8234288]

16. Owens DM, Romero MR, Gardner C, Watt FM. Suprabasal α6β4 integrin expression in epidermis results in enhanced tumorigenesis and disruption of TGFβ signalling. J Cell Sci. 2003; 116:3783–91. [PubMed: 12902406]

17. Janes SM, Watt FM. New roles for integrins in squamous cell carcinoma. Nat Rev Cancer. 2006; 6:175–83. [PubMed: 16498442]

18. Teige I, Backlund A, Svensson L, Kvist PH, Petersen TK, Kemp K. Induced keratinocyte hyperproliferation in α2β1 integrin transgenic mice results in systemic immune cell activation. Int Immunopharmacol. 2010; 10:107–14. [PubMed: 19840869]

19. Niculescu C, Ganguli-Indra G, Pfister V, Dupe V, Messaddeq N, De Arcangelis A, Georges-Labouesse E. Conditional ablation of integrin alpha-6 in mouse epidermis leads to skin fragility and inflammation. Eur J Cell Biol. 2011; 90:270–7. [PubMed: 20965608]

20. Arwert EN, Lal R, Quist S, Rosewell I, van Rooijen N, Watt FM. Tumor formation initiated by nondividing epidermal cells via an inflammatory infiltrate. Proc Natl Acad Sci USA. 2010; 107:19903–8. [PubMed: 21041641]

21. Marjolin, JN. Ulcère.. In: Bechet, editor. Dictionnaire de Medecine. Paris, France: 1828. p. 31-50.

22. Coussens LM, Werb Z. Inflammation and cancer. Nature. 2002; 420:860–7. [PubMed: 12490959]

23. Mueller MM. Inflammation in epithelial skin tumours: Old stories and new ideas. Eur J Cancer. 2006; 42:735–44. [PubMed: 16527478]

24. Moore RJ, Owens DM, Stamp G, Arnott C, Burke F, East N, Holdsworth H, Turner L, Rollins B, Pasparakis M, Kollias G, Balkwill F. Mice deficient in tumor necrosis factor-alpha are resistant to skin carcinogenesis. Nat Med. 1999; 5:828–31. [PubMed: 10395330]

25. Coussens LM, Tinkle CL, Hanahan D, Werb Z. MMP-9 supplied by bone marrow-derived cells contributes to skin carcinogenesis. Cell. 2000; 103:481–90. [PubMed: 11081634]

26. Girardi M, Oppenheim DE, Steele CR, Lewis JM, Glusac E, Filler R, Hobby P, Sutton B, Tigelaar RE, Hayday AC. Regulation of cutaneous malignancy by gammadelta T cells. Science. 2001; 294:605–9. [PubMed: 11567106]

27. Nibbs RJ, Gilchrist DS, King V, Ferra A, Forrow S, Hunter KD, Graham GJ. The atypical chemokine receptor D6 suppresses the development of chemically-induced skin tumors. J Clin Invest. 2007; 117:1884–92. [PubMed: 17607362]

28. Romero RM, Carroll JM, Watt FM. Analysis of cultured keratinocytes from a transgenic mouse model of psoriasis: effects of suprabasal integrin expression on keratinocytes adhesion, proliferation and terminal differentiation. Exp Dermatol. 1999; 8:53–67. [PubMed: 10206722]

29. Gregory SH, Wing EJ, Tweardy DJ, Shadduck RK, Lin H-S. Primary listerial infections are exacerbated in mice administered neutralizing antibody to macrophage colony-stimulating factor. J Immunol. 1992; 149:188–93. [PubMed: 1535085]

30. Cenci S, Weitzmann MN, Gentile MA, Aisa MC, Pacifici R. M-CSF neutralization and Egr-1 deficiency prevent ovariectomy-induced bone loss. J Clin Invest. 2000; 105:1279–87. [PubMed: 10792003]

31. Bachelor MA, Lu Y, Owens DM. L-3-phosphoserine phosphatase (PSPH) regulates cutaneous squamous cell carcinoma proliferation independent of L-serine biosynthesis. J Dermatol Sci. 2011; 63:164–72. [PubMed: 21726982]

32. Trickett A, Kwan YL. T cell stimulation and expansion using anti-CD3/CD28 beads. J Immunological Meth. 2003; 275:251–5.

33. Maurer M, von Stebut E. Macrophage inflammatory protein-1. Int J Biochem Cell Biol. 2004; 36:1882–6. [PubMed: 15203102]

34. Biswas SK, Sodhi A. Effect of monocyte chemoattractant protein-1 on murine bone marrow cells: proliferation, colony-forming ability and signal transduction pathway involved. Int J Immunopathol Pharmacol. 2002; 15:183–94. [PubMed: 12575918]

35. Ruddy MJ, Shen F, Smith JB, Sharma A, Gaffen SL. Interleukin-17 regulates expression of the CXC chemokine LIX/CXCL5 in osteoblasts: implications for inflammation and neutrophil recruitment. J Leukoc Biol. 2004; 76:135–44. [PubMed: 15107456]

36. Vieira SM, Lemos HP, Grespan R, Napimoga MH, Dal-Secco D, Freitas A, Cunha TM, Verri WA, Souza-Junior DA, Jamur MC, Fernandes KS, Oliver C, Silva JS, Teixeira MM, Cunha FQ. A crucial role for TNF-alpha in mediating neutrophil influx induced by endogenously generated or

exogenous chemokines, KC/CXCL1 and LIX/CXCL5. Br J Pharmacol. 2009; 158:779–89. [PubMed: 19702783]

37. Douglass TG, Driggers L, Zhang JG, Hoa N, Delgado C, Williams CC, Dan Q, Sanchez R, Jeffes EW, Wepsic HT, Myers MP, Koths K, Jadus MR. Macrophage colony stimulating factor: Not just for macrophages anymore! A gateway into complex biologies. Int Immunopharm. 2008; 8:1354–76.
38. Stumpfova M, Ratner D, Desciak EB, Eliezri YD, Owens DM. The immunosuppressive surface ligand CD200 augments the metastatic capacity of squamous cell carcinoma. Cancer Res. 2010; 70:2962–72. [PubMed: 20332223]
39. Rosenblum MD, Woodliff JE, Madsen NA, McOlash LJ, Keller MR, Truitt RL. Characterization of CD200-receptor expression in the murine epidermis. J Invest Dermatol. 2005; 125:1130–8. [PubMed: 16354182]
40. Murphy PM. Neutrophil receptors for interleukin-8 and related CXC chemokines. Semin Hematol. 1997; 34:311–8. [PubMed: 9347581]
41. Clark RA, Huang SJ, Murphy GF, Mollet IG, Hijnen D, Muthukuru M, Schanbacher CF, Edwards V, Miller DM, Kim JE, Lambert J, Kupper TS. Human squamous cell carcinomas evade the immune response by down-regulation of vascular E-selectin and recruitment of regulatory T cells. J Exp Med. 2008; 205:2221–34. [PubMed: 18794336]
42. Badoual C, Hans S, Rodriguez J, Peyrard S, Klein C, Agueznay NEH, Mosseri V, Laccourreye O, Bruneval P, Fridman WH, Brasnu DF, Tartour E. Prognostic value of tumor-infiltrating CD4+ T-cell subpopulations in head and neck cancers. Clin Cancer Res. 2006; 12:465–72. [PubMed: 16428488]
43. Priceman SJ, Sung JL, Shaposhnik Z, Burton JB, Torres-Collado AX, Moughon DL, Johnson M, Lusis AJ, Cohen DA, Iruela-Arispe ML, Wu L. Targeting distinct tumor-infiltrating myeloid cells by inhibiting CSF-1 receptor: combating tumor evasion of antiangiogenic therapy. Blood. 2010; 115:1461–71. [PubMed: 20008303]
44. Gabrilovich DI, Nagaraj S. Myeloid-derived suppressor cells as regulators of the immune system. Nat Rev Immunol. 2009; 9:162–74. [PubMed: 19197294]
45. Pixley FJ, Stanley ER. CSF-1 regulation of the wandering macrophage: complexity in action. Trends Cell Biol. 2004; 14:628–38. [PubMed: 15519852]
46. Menke J, Hsu M-Y, Byrne KT, Lucas JA, Rabacal WA, Croker BP, Zong XH, Stanley ER, Kelley VR. Sunlight triggers cutaneous lupus through a CSF-1 dependent mechanism in MRL-*Fas*^{lpr} mice. J Immunol. 2008; 181:7367–79. [PubMed: 18981160]
47. Huang B, Pan PY, Li Q, Sato AI, Levy DE, Bromberg J, Divino CM, Shen SH. Gr-1+CD115+ immature myeloid suppressor cells mediate the development of tumor-induced T regulatory cells and T-cell anergy in tumor-bearing host. Cancer Res. 2006; 66:1123–31. [PubMed: 16424049]
48. Movahedi K, Guilliams M, Van den Bossche J, Van den Bergh R, Gysemans C, Beschin A, De Baetselier P, Van Ginderachter JA. Identification of discrete tumor-induced myeloid-derived suppressor cell populations with distinct T cell-suppressive activity. Blood. 2008; 111:4233–44. [PubMed: 18272812]

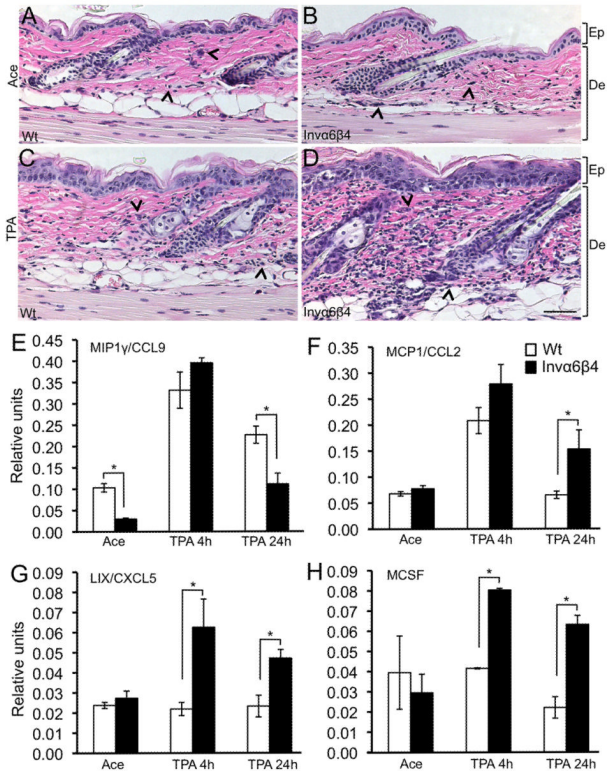

Fig. 1.

Modulated infiltrate and cytokine secretion in TPA-treated Invα6β4 transgenic skin. (**A-D**) Histological sections from acetone vehicle- (top row) or TPA-treated (bottom row) Wt (left panels) and Invα6β4 (right panels) mouse skin stained with H&E. Arrow heads point to dermal infiltrative cells. Scale bar: 50 μm. Abbreviations: De, dermis; Ep, epidermis. (**E-H**) Bar graphs depicting the relative units of CCL9, CXCL5, MCP1 or M-CSF compared between acetone vehicle- or TPA-treated Wt and Invα6β4 mouse skin. *- $p < 0.05$ (Student's *t* test).

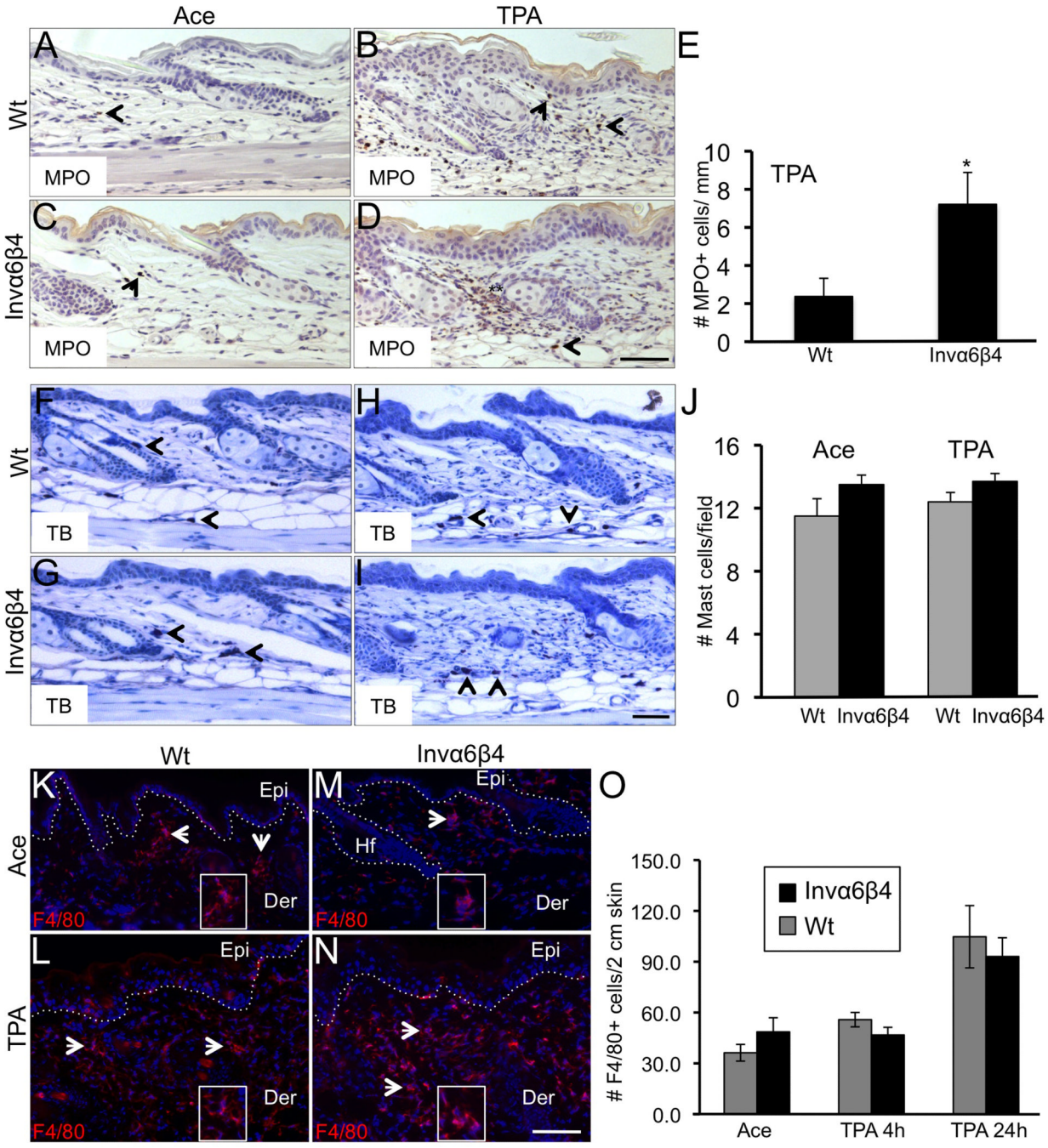

Fig. 2.

Analysis of MPO$^+$, mast cell and macrophage skin infiltrates in response to TPA. (**A-D**) Immunodetection (arrowheads) of MPO$^+$ infiltrating inflammatory cells in histological sections of acetone- (left panels) or TPA-treated (right panels) Wt (top row) or Invα6β4 (bottom row) mouse skin. Scale bar: 20 μm. (**E**) Bar graph depicting the average number of MPO$^+$ dermal cells per mm of skin in TPA-treated Wt versus Invα6β4 mice, 3 mice per group. *- p = 0.036 (Student's *t* test). (**F-I**) Toluidine blue stain detection of infiltrating mast cells (arrowheads) in histological sections of acetone- (left panels) or TPA-treated (right panels) Wt (top row) or Invα6β4 (bottom row) mouse skin. Scale bar: 20 μm. (**J**) Bar graph depicting the average number of dermal mast cells per mm of skin in TPA-treated Wt versus

Invα6β4 mice, 3 mice per group. (**K-N**) Immunodetection (arrowheads) of F4/80$^+$ dermal macrophages in histological sections of acetone- (top row) or TPA-treated (bottom row) Wt (left panels) or Invα6β4 (right panels) mouse skin. Scale bar: 20 μm. Hashed lines demarcate the epidermal-dermal junction and boxes contain 4X magnification insets of F4/80$^+$ dermal cells. Abbreviations: Epi, epidermis; Der, dermis; Hf, hair follicle. (**O**) Bar graph depicting the average number of F4/80$^+$ macrophages per 2 cm of skin in TPA-treated Wt versus Invα6β4 mice, 3 mice per group.

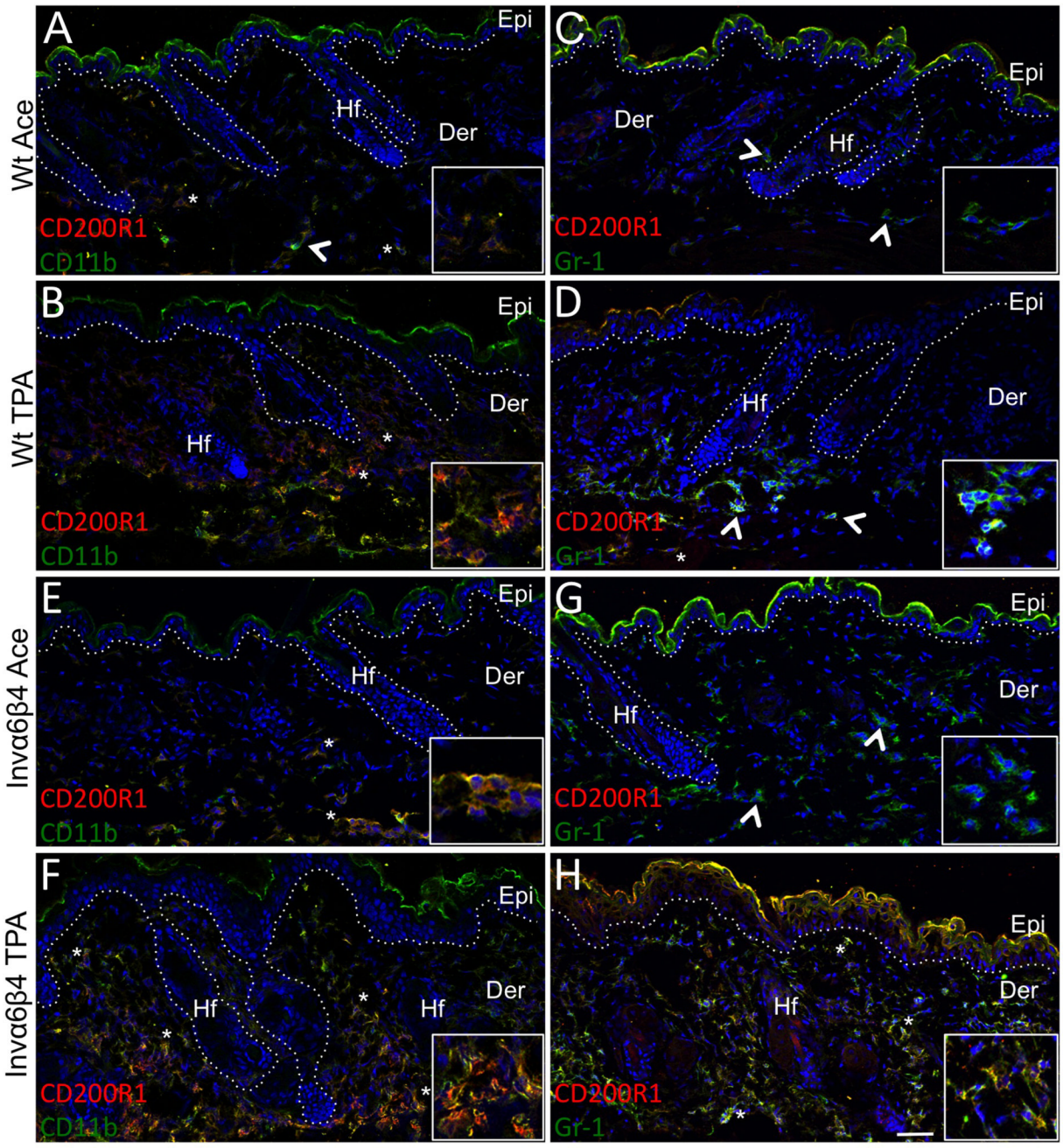

Fig. 3.

Immunosuppressive myeloid cells preferentially infiltrate Invα6β4 skin. (**A-H**) Immunolabeling of CD200R1 in conjunction with either CD11b (left panels) or Gr-1 (right panels) in histological sections from acetone vehicle- or TPA-treated (24 hr) Wt and Invα6β4 mouse skin. Arrowheads point to $CD11b^{+}$ or $Gr\text{-}1^{+}$ single-stained and asterisks indicate $CD200R1^{+}CD11b^{+}$ or $CD200R1^{+}Gr\text{-}1^{+}$ double-stained dermal infiltrative cells. Hashed lines demarcate the epidermal-dermal junction and boxes contain 4X magnification insets of immunopositive dermal cells. Abbreviations: Epi, epidermis; Der, dermis; Hf, hair follicle. Scale bar: 50 μm.

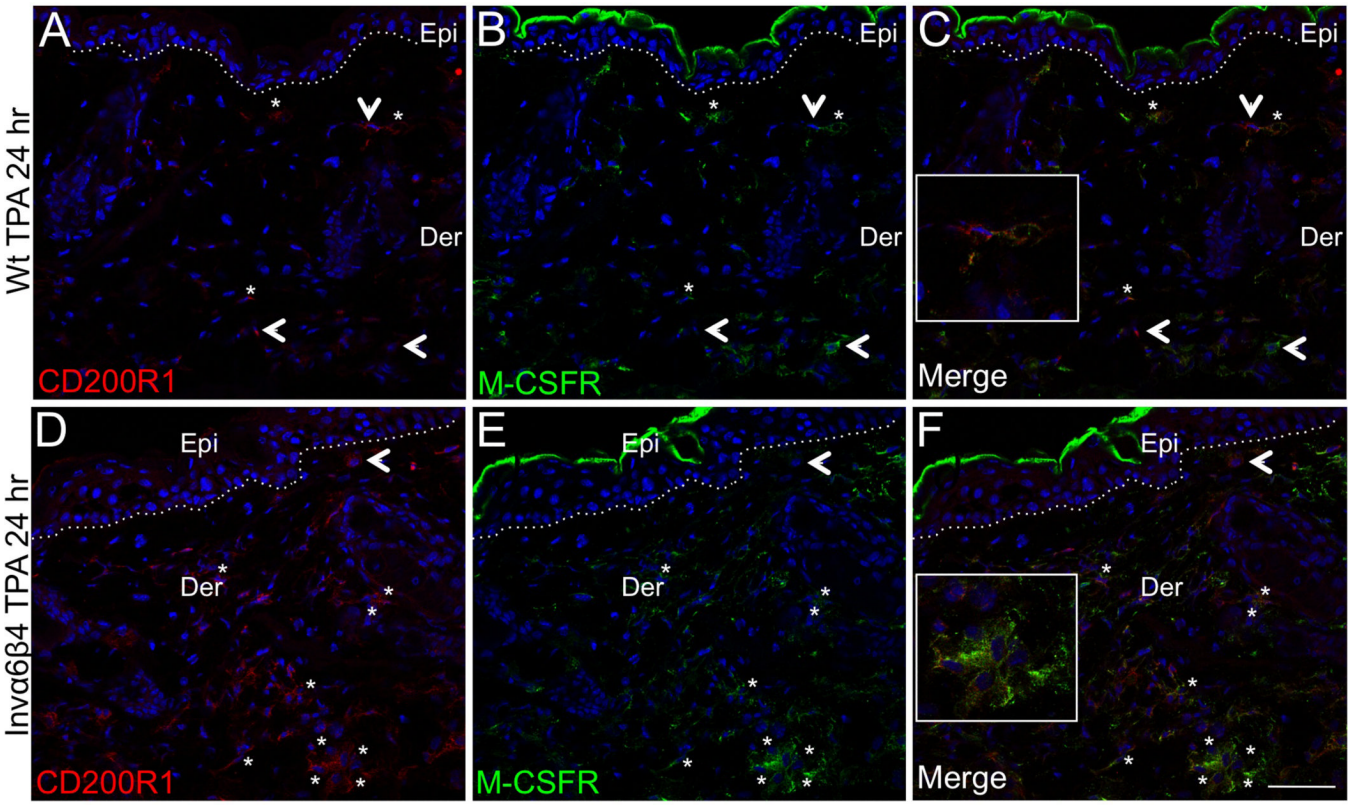

Fig. 4.

M-CSF receptor expression in skin infiltrative cells. (**A-F**) Immunolabeling of CD200R1 (left panels) in conjunction with M-CSFR (middle panels) in histological sections from TPA-treated Wt (top row) or Invα6β4 (bottom row) mouse skin. Merged images (right panels) confirm CD200R1 or M-CSFR single-stained cells (arrowheads) and asterisks (*) indicate $CD200R1^{+}MCSFR^{+}$ double-stained dermal infiltrative cells. Hashed lines demarcate the epidermal-dermal junction and boxes contain 4X magnification insets of immunopositive dermal cells (**C** and **F**). Abbreviations: Epi, epidermis; Der, dermis. Scale bar: 50 μm.

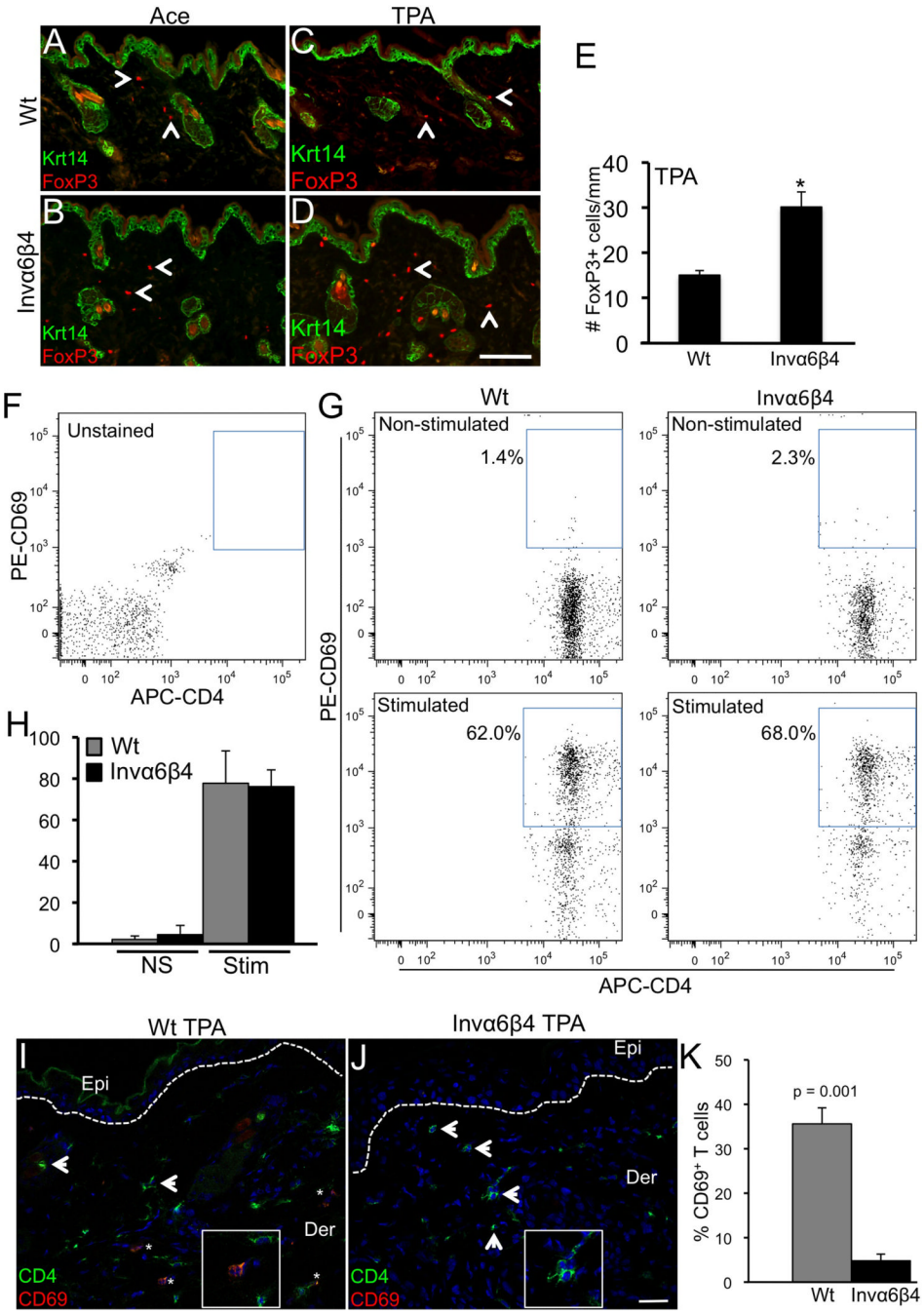

Figure 5.

TPA-induced Foxp3$^+$ cell infiltration and CD4$^+$ T lymphocyte suppression in Invα6β4 skin. (**A-D**) Immunodetection of FoxP3 and Krt14 in histological sections from acetone vehicle- (left panels) or TPA-treated (right panels) Wt (top row) and Invα6β4 (bottom row) mouse skin. Arrow heads point to FoxP3$^+$ dermal infiltrative cells. Scale bar: 50 μm. (**E**) Bar graph depicting the average number of FoxP3$^+$ cells per mm of skin from 3 mice per group. *- p = 0.001 (Student's *t* test). (**F** and **G**) FACS dot plots showing a typical array of CD4$^+$ (x-axis) versus CD69$^+$ (y-axis) T lymphocytes detected in either non-stimulated or CD3/CD28-stimulated peripheral blood samples isolated from Wt or Invα6β4 mice. Blue box depicts the gate for CD4$^+$CD69$^+$ activated T lymphocytes for each plot. (**H**) Bar graph depicting the

average number of $CD4^+CD69^+$ T lymphocytes from non-stimulated (NS) or CD3/CD28-stimulated (Stim) peripheral blood samples isolated from Wt or Invα6β4 mice, n = 3 mice per group and error bars represent standard deviation. (**I** and **J**) Immunodetection of CD4 (green) and CD69 (red) T lymphocytes in histological sections from TPA-treated (24 hr) Wt (left panel) and Invα6β4 (right panel) mouse skin. Arrowheads point to $CD4^+$ infiltrative T cells and asterisks (*) designate $CD4^+CD69^+$ cells. Hashed lines demarcate the epidermal-dermal junction and boxes contain 4X magnification insets of immunopositive dermal cells. Abbreviations: Epi, epidermis; Der, dermis. Scale bar: 50 μm. (**K**) Bar graph depicting the percentage of $CD4^+$ T lymphocytes co-expressing the activation marker CD69 in Wt versus Invα6β4 skin 24 hr following TPA treatment, n = 3 mice per group and error bars represent standard deviation.

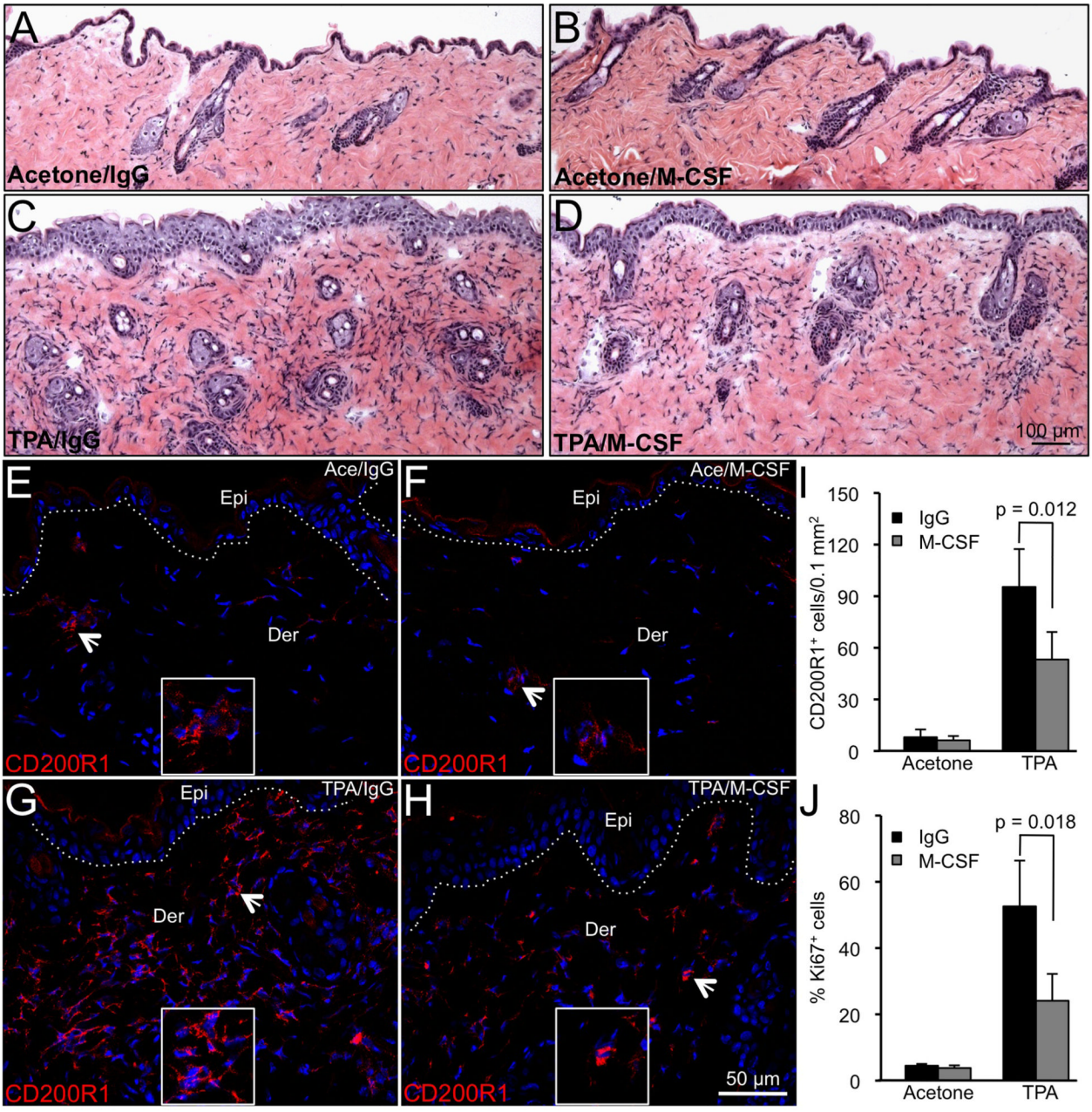

Figure 6.

M-CSF neutralization suppresses TPA-induced MDSC recruitment and epidermal proliferation. (**A-H**) Representative images of skin sections stained with H&E (**A-D**) or probed with CD200R1 antibodies (**E-H**) from Invα6β4 mice receiving acetone vehicle (**A,B** and **E,F**) or TPA (**C,D** and **G,H**) followed by IgG control (**A,C** and **E,G**) or M-CSF (**B,D** and **F,H**) antibody injection. (**E-H**) Arrowheads point to $CD20R1^+$ infiltrative cells. Hashed lines demarcate the epidermal-dermal junction and boxes contain 4X magnification insets of $CD200R1^+$ dermal cells. Abbreviations: Epi, epidermis; Der, dermis. (**I** and **J**) Bar graphs depicting the average number of $CD200R1^+$ infiltrating cells per 0.1 mm^2 area of skin (**I**) or the percentage of $Ki67^+$ basal epidermal keratinocytes (**J**) in each Invα6β4 treatment group. Error bars represent standard deviation from 2 mice per treatment group.